Correlation between the Magnetic and DC resistivity studies of Cu substituted Ni and Zn in Ni-Zn ferrites

D. Parajuli[1, 2]***, N. Murali**[3]**, K. Samatha**[4]

[1]Research Center for Applied Science and Technology (RECAST), Tribhuvan University, Kathmandu- 44613, Nepal

[2]Tri-Chandra Multiple Campus, Tribhuvan University, Ghantaghar, Kathmandu, Nepal

[3]Department of Physics, College of Engineering (A), Andhra University, Visakhapatnam-530003, India

[4]Department of Physics, Andhra University, Visakhapatnam-530003, India

*Email: deepenparaj@gmail.com

ABSTRACT

Cu substituted $Ni_{0.5-x}Cu_xZn_{0.5}Fe_2O_4$ (x = 0, 0.05, 0.1, 0.15 and 0.2) samples is synthesized using the sol-gel auto-combustion process. They have a cubic spinel structure with crystallite size in the range of 29.01–42.68 nm. The increment in the copper content increases the DC conductivity. The electrical resistivity decrease with an increase in the temperature i.e. it has a negative temperature coefficient with resistance similar to semiconductors. The remnant ratios R obtained from VSM show their isotropic nature forming single domain ferrimagnetic particles. The results are compared with $Ni_{0.5}Cu_xZn_{0.5-x}Fe_2O_4$ (x = 0 to 0.25). The resultant material Cu substituted Zn is more significant than that of Ni as indicated by its results and previous literature.

1. Introduction

Microwave devices, magnetic recording, coating, etc. are the major applications of Ni-Zn spinel ferrites [1-3]. Their crystal structure supports them in tuning their microstructural and electromagnetic properties which are necessary for many advanced applications. They have $M^{2+}Fe_2^{3+}O_4^{2-}$ composition with transitional metal (M) in tetrahedral and Fe on the octahedral region of the nano ferrite. A vigorous study on their structural and magnetic properties with doping of several elements in Ni-Cu-Zn ferrites is increasing day by day [4-6]. The core of Rotary Dy, transformer, and magnetic induction uses these types of ferrites. In some cases, the density, porosity, the interactions among the particles with canting effects affect their magnetic properties. Recently, we have studied the effect of Cu substitution on magnetic and DC electrical resistivity of Ni-Zn ferrites $Ni_{0.5}Zn_{0.5-x}Cu_xFe_2O_4$ ($x = 0$, 0.1, 0.2, 0.3, and 0.4) [7], structural and morphological study of Cu substituted Ni/Zn in Ni-Zn ferrite comparatively [8, 9], Cd substituted Ni-Zn ferrites [10] and Ni substituted Co Zn ferrites [11]. They all have spinel structures with semiconducting nature.

In the present study, Cu substituted nickel ferrites are prepared by the sol-gel method, and compare their magnetic and DC electrical properties with Cu substituted Zn in Ni-Zn ferrites synthesized from the citrate gel route [12, 13]. The Cu substituted Zn in Ni-Zn ferrites is appropriate for Multilayer Chip Inductor (MLCI) as magnetic material.

2. Methodology

A. Materials

The sol-gel method was used for the preparation of $Ni_{0.5}Zn_{0.5-x}Cu_xFe_2O_4$ ($x = 0$, 0.1, 0.2, 0.3, and 0.4). The nitrates of Nickel, Copper, Zinc, Iron and citric acid with 99.99% purity were used as starting materials and mixed in a 1:1 ratio. The solution was made clear with double distilled water. Liquid ammonia was added dropwise with magnetic stirring at 100°C for 4 hrs. for getting the neutral solution after it was made neutral by adding liquid ammonia. The solution was then decanted and dried for 40 hrs. at room temperature. The resultant was powdered and sintered in a muffle furnace at 800 °C for 4 h at 5°/min.

B. Characterizations

The structure of $Ni_{0.5}Zn_{0.5-x}Cu_xFe_2O_4$ ($x = 0$, 0.1, 0.2, 0.3, and 0.4) was studied with the help of an X-ray diffractometer (Rigaku Miniflex II) with CuKα radiation of 1.5406 Å. The morphological and compositional study was made with TESCAN, MIRA II LMH SEM, and attached Inca Oxford EDX. The functional group and room temperature magnetic properties were studied with FT-IR and EZ-VSM- models respectively. The disc-shaped pellets were made with the help of a hydraulic system of 5 tons of pressure incorporating a few drops of polyvinyl alcohol as a binder. Their flat surfaces were polished with gold to use as electrodes after being sintered at 800°C in a muffle furnace and used for the study of DC resistivity in two probe systems.

3. Results and Discussions

A. Magnetic properties

EZ-VSM used for the magnetic characterization of $Ni_{0.5}Zn_{0.5-x}Cu_xFe_2O_4$ ($x = 0$, 0.1, 0.2, 0.3 and 0.4). Ferrites have higher resistivity due to unequal antimagnetic moments giving rise to higher spontaneous magnetization. Moreover, they have a negative exchange integral affected by an interatomic distance which obstructs the flow of electrons [14]. However, their saturation permeability, coercivity, susceptibility, Curie temperature, etc. are affected by the density of ions in their respective interstitial sites and their structure determines the hysteresis loop's shape, resistivity, ac conductivity, and dielectric constant. The doping of either magnetic or nonmagnetic extrinsic elements changes their property accordingly. The magnetic saturation, coercivity, etc. are calculated from their hysteresis curves as shown in figure 1. The obtained values of Ms and Hc are listed in Table 1 [15].

Table 1: Ms and Hc of $Ni_{0.5-x}Cu_xZn_{0.5}Fe_2O_4$ (x = 0.0, 0.05, 0.1, 0.15 and 0.2) ferrites

Concentration (x)	Ms (emu/g)	Hc (Oe)
0.0	73.26	45.36
0.05	80.66	60.62
0.1	83.86	84.45
0.15	56.05	65.26
0.2	46.32	51.48

From table 1, Ms increases up to (x ≤ 0.1) and then starts decreasing with Cu^{2+} concentration. This is due to the distribution of cations and exchange interaction. On adding copper ions to the Nickel-Zinc mixture, they exchange a few magnetic ions Fe^{3+} and Ni^{2+} in A and B- sites. The AB interaction is then increased thereby resisting antiparallel spin which ultimately raises the magnetic saturation [16]. According to Weiss's Molecular field theory, the mixed interaction (A-B and B-A) is more than similar A-A and B-B interaction resulting from the hysteresis loop [17].

The increment of nonmagnetic Cu ion in place of Zn ion decreases saturation magnetization. The occupancy of the B site by Cu ion helps Fe^{3+} ions migrate to the A-site thereby reducing magnetization in the B site and increasing in the A site. The total magnetization is obtained using Neel's [18] law, according to which M=$|M_B − M_A|$. So, the Cu substituted Zinc effectively works in changing the magnetic properties of the sample than Nickel.

B. DC Electrical Resistivity

There is a rapid, then steady and finally constant decrease of DC resistivity of Cu substituted Nickel in Ni-Zn ferrites nanoparticles with Cu concentration [19] as shown in DC resistivity vs. temperature for the Cu substituted Ni-Zn ferrite of figure 3. A straight line is obtained from the $\log_e\rho$ vs. 1000/T graph showing the semiconducting nature of the ferrites under consideration. The temperature variation of DC electrical resistivity of $Ni_{0.5}Zn_{0.5−x}Cu_xFe_2O_4$ ferrite samples as in figure 4 indicates that all the samples have semiconducting properties.

Further, the temperature-dependent resistivity varied larger with the concentration of Cu ion and seems more effective for x=0.15 in the case of Cu substituted zinc in Ni-Zn ferrite. So, the resistive property is changed effectively in Cu substituted zinc in Ni-Zn ferrite than that in Cu substituted nickel.
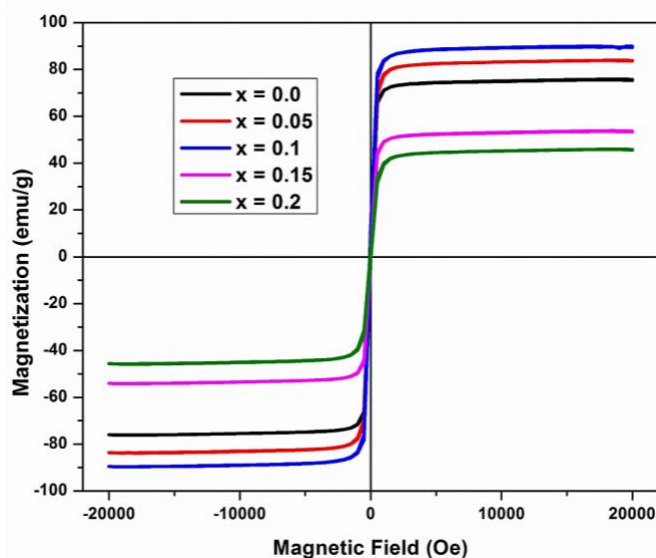

Figure 1: Hysteresis curves of $Ni_{0.5-x}Cu_xZn_{0.5}Fe_2O_4$ (x = 0.0, 0.05, 0.1, 0.15 and 0.2) ferrite NPs at room temperature
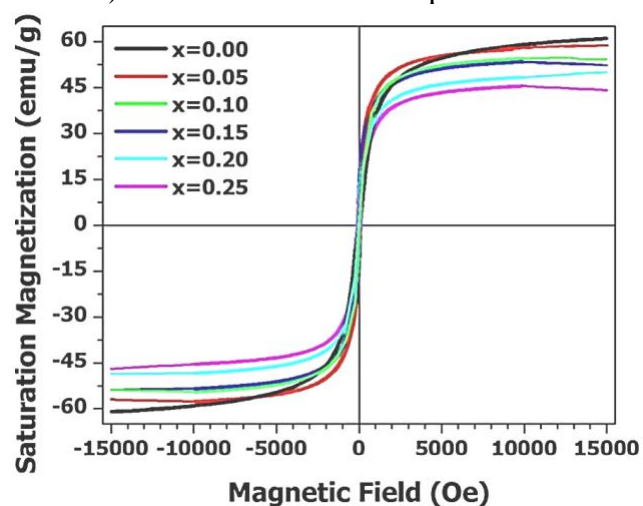
Figure 2: Hysteresis curves of $Ni_{0.5}Zn_{0.5−x}Cu_xFe_2O_4$ (x=0.00 to 0.25) at room temperature [12]

C. Activation energy calculation

The slope of the tangents on the plot of 1000/T versus $\log_e\rho$ of $Ni_{0.5}Zn_{0.5−x}Cu_xFe_2O_4$ is used for the calculation of their activation energies where we use the Arrhenius relation

incorporating the dynamism of hopping charge carriers due to temperature [19] as:

$$\rho = \rho_o e^{\left(\frac{\Delta E}{KT}\right)} \qquad (1)$$

where, ρ and ρ_o are the dc electrical resistivity at temperature T and absolute zero. ΔE and K are the activation energy and the Boltzmann constant. The activation energies obtained are plotted against the concentration of the Cu in $Ni_{0.5}Zn_{0.5-x}Cu_xFe_2O_4$ are shown in figure 5.

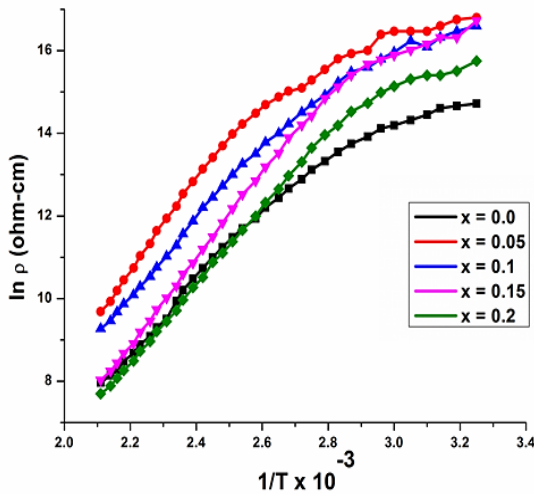Figure 3: Temperature dependence of DC resistivity of $Ni_{0.5-x}Cu_xZn_{0.5}Fe_2O_4$ (x = 0.0, 0.05, 0.1, 0.15 and 0.2) ferrites
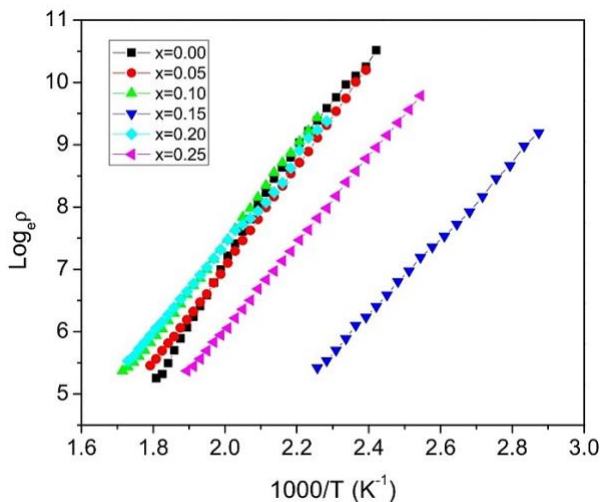
Figure 4: 1000/T versus $\log_e\rho$ of $Ni_{0.5}Zn_{0.5-x}Cu_xFe_2O_4$ samples (x = 0.00 to 0.25) [13]

The variation in resistivity of the samples is according to the Verwey and de Boer hopping mechanism in which the electrons of the same element jump at their

different valence states. As a result, $Fe^{2+}\Leftrightarrow Fe^{3+}$ hopping is raised for higher sintering temperature as more Fe^{2+} ions. The $Ni^{2+} \Leftrightarrow Ni^{3+}$ and $Cu^{3+} \Leftrightarrow Cu^{2+}$ hopping can also take place simultaneously [21].
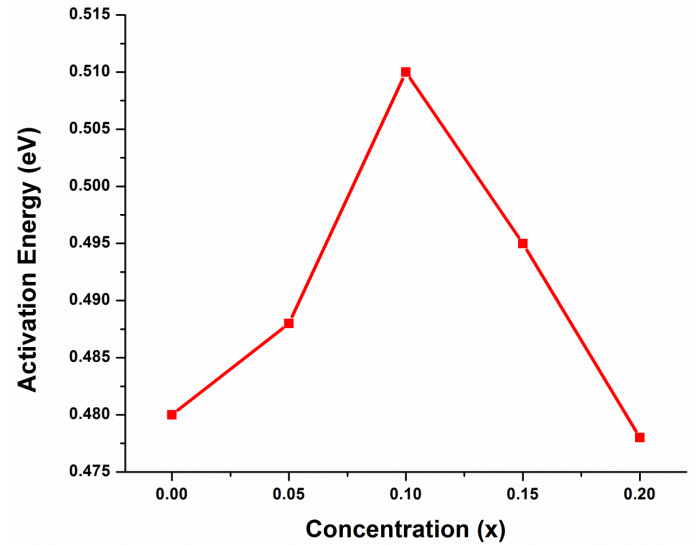
Figure 5: Activation energies Vs. Concentration (x) of the $Ni_{0.5-x}Cu_xZn_{0.5}Fe_2O_4$ (x = 0.0, 0.05, 0.1, 0.15 and 0.2)
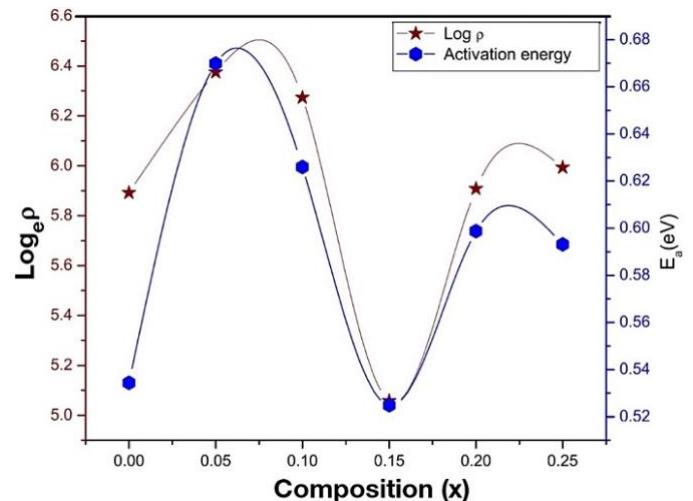
Figure 6: Cu concentration vs. $\log_e\rho$ & E_a of $Ni_{0.5}Zn_{0.5-x}Cu_xFe_2O_4$ (x = 0.00 to 0.25) [13]

Figure 6 shows the variation of activation energies and DC resistivity with Cu substituted zinc concentration in $Ni_{0.5}Zn_{0.5-x}Cu_xFe_2O_4$ nanocrystalline ferrite samples (x = 0.00 to 0.25). From the Figure, it is observed that the

activation energies and resistivities of the samples are fluctuated more than that in Cu substituted nickel in NiZn ferrites but in the range of 0.53 eV to 0.67 eV.

4. Conclusion

The structures of the nanocrystalline $Ni_{0.5-x}Cu_xZn_{0.5}Fe_2O_4$ (x = 0.0, 0.05, 0.1, 0.15, and 0.2) ferrite NPs were synthesized by Sol-gel auto-combustion method and confirmed their structure to have single-phase cubic spinel ferrite with the help of XRD and FTIR. The magnetic measurements show that saturation magnetization, coercive forces, and activation energy are highest at x = 0.1. While the conductivity is lowest at x=0.05 in the case of Cu substituted nickel. The Zinc content effectively works in changing the magnetic properties of Nickel. Both have isotropic magnetism. In both cases, the electrical resistivity decrease with an increase in the temperature i.e. it has a negative temperature coefficient with resistance similar to semiconductors. The activation energies are varied more in the range 0.53 eV to 0.67 eV in Cu substituted zinc than that in the range 0.42 to 0.51 eV. The variation in Cu substituted nickel and Cu substituted zinc synthesized by two different processes are due to their different (a) density and porosity (b) super-exchange interactions (bond angles and lengths) and (c) spin canting effects. The values agree well with our and other previous calculations. The tuning properties that arise with Cu doping in place of zinc and nickel separately have a significant role in various devices like multilayer chip inductors, magnetic cores, etc.

References

[1] Yu S, Wu G, Gu X, Wang J, Wang Y, Gao H, et al., Magnetic and pH-sensitive nanoparticles for antitumor drug delivery, Colloids Surf. 103 (2013) 15–22.
https://doi.org/10.1016/j.colsurfb.2012.10.041

[2] Y. Tejabhiram, R. Pradeep, A. T. Helen, C. Gopalakrishnan, C. Ramasamy, Synthesis and magnetic properties of gadolinium substituted zinc ferrites, Mater. Res. Bull. 60 (2014) 778–82.
https://doi.org/10.1016/j.matlet.2016.11.083

[3] D. K. Jha, M. Shameem, A. B. Patel, A. Kostka, P. Schneider, A. Erbe, P. Deb, Simple synthesis of superparamagnetic magnetite nanoparticles as highly efficient contrast agent, Mater. Lett. 95 (2013)186–189.
https://doi.org/10.1016/j.matlet.2012.12.096

[4] S. Kenouche, J. Larionova, N. Bezzi, Y. Guari, N. Bertin, M. Zanca, L. Lartigue, M. Cieslak, C. Godin, C. Goze-Bac, NMR investigation of functionalized magnetic nanoparticles Fe_3O_4 as T1–T2 contrast agents, Powder Technol. 225 (2014) 60–5.
https://doi.org/10.1016/j.powtec.2013.07.038

[5] F. Geinguenaud, I. Souissi, R. Fagard, L. Motte, Y. Lalatonne, Electrostatic assembly of a DNA superparamagnetic nano-tool for simultaneous intracellular delivery and in situ monitoring, Nanomed. Nanotechnol. Biol. Med. 8 (2012)1106–15.
https://doi.org/10.1016/j.nano.2011.12.010

[6] Ji Hyun Min, Mi-Kyung Woo, Ha Young Yoon, Jin Woo Jang, Jun Hua Wu, Chae-Seung Lim, Young Keun Kim, Isolation of DNA using magnetic nanoparticles coated with dimercapto succinic acid, Anal. Biochem. 447 (2014) 114–8.
https://doi.org/10.1016/j.ab.2013.11.018

[7] A. Drmota, J. Koselj, M. Drofenik, A. Znidarsic, Electromagnetic wave absorption of polymeric nanocomposites based on ferrite with spinel and hexagonal crystal structure, J. Magn. Magn. Mater 324(2012)1225–9.
https://doi.org/10.1016/j.jmmm.2011.11.015

[8] Chandramouli, K., Rao, P.A., Suryanarayana, B. *et al.* Effect of Cu

substitution on magnetic and DC electrical resistivity properties of Ni–Zn nanoferrites. J Mater Sci: Mater Electron 32(2021)15754–15762. https://doi.org/10.1007/s10854-021-06127-7

[9] D. Parajuli, K. Samatha. Structural analysis of Cu substituted Ni/Zn in Ni-Zn Ferrite. *BIBECHANA,* 18 (1) (2020) 128-133. https://doi.org/10.3126/bibechana.v18i1.29474

[10] D. Parajuli, K. Samatha, Morphological Analysis of Cu substituted Ni/Zn in Ni-Zn Ferrites, *Journal of Physical Science, BIBECHANA* (2020) 18 (2) (2021) 80-86.https://doi.org/10.3126/bibechana.v18i2.34383

[11] D. Parajuli, Vemuri Raghavendra, B. Suryanarayana, P. Anantha Rao, N. Murali, P.V.S.K. Phanidhar Varma, R. Giri Prasad, Y. Ramakrishna, K. Chandramouli, Cadmium substitution effect on structural, electrical and magnetic properties of Ni-Zn nano ferrites. Results in Physics, 23(2021) 103947.https://doi.org/10.1016/j.rinp.2021.103947

[12] D. Parajuli, N. Murali, and K. Samatha; Structural, Morphological, and Magnetic Properties of Nickel Substituted Cobalt Zinc Nanoferrites at Different Sintering Temperature, JNPS, 7 (2)(2021) 24-32. https://doi.org/10.3126/jnphyssoc.v7i2.38619

[13] D. Venkatesh, B. B. V. S. Vara Prasad, K. V. Ramesh, M. N. V. Ramesh, Magnetic Properties of Cu2+ Substituted Ni–Zn Nano-Crystalline Ferrites Synthesized in Citrate-Gel Route, J. Inorg Organomet. Polym Mater. 30(2020)2057–2066. https://doi.org/10.1007/s10904-019-01419-2

[14] D. Venkatesh, K. V. Ramesh, Structural and electrical properties of Cu-doped Ni–Zn nanocrystalline ferrites for MLCI applications, Mod. Phys. Lett. B 31 (33) (2017)1750318. http://doi.org/10.1142/S0217984917503183

[15] Li Y., Zhang C., Liu Y., Tang S., Chen G., Zhang R. and Tang X.Coke formation on the surface of Ni/HZSM-5 and Ni-Cu/HZSM-5 catalysts during bio-oil hydrodeoxygenation, Fuel, 189 (2017)23-31. https://doi.org/10.1016/j.fuel.2016.10.047

[16] S. R. Jain, K. C. Adiga and V. R. Pai Verneker, "A New Approach to Thermochemical Calculations of Condensed Fuel-Oxidizer Mixtures," Combust. Flame, 40(1981)71-79. http://doi.org/10.1016/0010-2180(81)90111-5

[17] Klung H, Alexander L. X-ray Diffraction Procedures for Polycrystalline and Amorphous Materials, New York: Wiley;1962. https://doi.org/10.1002/bbpc.19750790622

[18] Reed JS. Principles of Ceramic Processing New York: John Wiley & Sons; 1996. pp. 443.

[19] Bushra Praveen, Mahmood-ul-Hassan, Zeeshan Khalid, Saira Riaz, Shahzad Naseem, Room-temperature ferromagnetism in Ni-doped TiO_2 diluted magnetic semiconductor thin films, Journal of Applied Research and Technology-(2017) 214. https://doi.org/10.1016/j.jart.2017.01.009

[20] Kumar S, Kumar P, Singh V, Kumar Mandal U, Kumar Kotnala, Synthesis, characterization and magnetic properties of monodisperse Ni, Zn-ferrite nanocrystals, J. Magn. Magn. Mater. 379(2015)50–7. https://doi.org/10.1016/j.jmmm.2014.12.006

[21] Andreev VG, Menshova SB, Klimov AN, Vergazov RM. The influence of basic composition and microstructures on the properties of Ni–Zn ferrite radio-absorbing materials, J. Magn. Magn. Mater.393(2015)569–73. https://doi.org/10.1016/j.jmmm.2015.06.030

[22] Batoo KM, Ansari MS. Low temperature-fired Ni-Cu-Zn ferrite

nanoparticles through auto-combustion method for multilayer chip inductor applications, Nanoscale Res. Lett. 7(1)(2012)1–14.
https://doi.org/10.1186/1556-276X-7-112